Electrical Double Layer Structure in Ionic Liquids and its Importance for Supercapacitor, Battery, Sensing and Lubrication Applications

Debbie S. Silvester[1,*] Rabia Jamil,[1] Simon Doblinger,[1] Yunxiao Zhang,[2] Rob Atkin,[2] Hua Li[2,3]

1: *School of Molecular and Life Sciences, Curtin University, GPO Box U1987, Perth, 6845, WA, Australia.*
2: *School of Molecular Sciences, The University of Western Australia, Perth, Western Australia, Australia.*
3: *Centre for Microscopy, Characterisation and Analysis, The University of Western Australia, Perth, Western Australia, Australia*

*Corresponding author: Debbie S. Silvester *(d.silvester-dean@curtin.edu.au)*
Tel.: +61-08-9266-7148; Fax: +61-08-9266-2300

Invited Perspective article for the Journal of Physical Chemistry C

Abstract:

Ionic Liquids (ILs) have become highly popular solvents over the last two decades in a range of fields, especially in electrochemistry. Their intrinsic properties include high chemical and thermal stability, wide electrochemical windows, good conductivity, high polarity, tuneability, and good solvation properties, making them ideal as electrochemical solvents for different applications. At charged surfaces such as electrodes, an electrical double layer (EDL) forms when exposed to a fluid. IL ions form denser EDL structures compared to conventional solvent/electrolyte systems, which can cause differences in the behaviour for electrochemical applications. This Perspective article discusses some recent work (over the last 3 years) where the structure of the EDL in ILs has been examined and found to influence the behaviour of supercapacitors, batteries, sensors and lubrication systems that employ IL solvents. More fundamental work is expected to continue in this area, which will inform the design of solvents for use in these applications and beyond.

Keywords:

Ionic liquids; room temperature ionic liquids, electrical double layer; electrochemistry; interface; applications.

1. Introduction – Structure of the Electrical Double Layer in Ionic Liquids

Ionic liquids (ILs) are pure salts that have melting points lower than 100ºC, and room temperature ionic liquids (RTILs) – a subclass – are liquids below 25ºC IL properties, such as high chemical and thermal stability, good conductivity, wide electrochemical windows, good solvation, and tuneability, have resulted in significant fundamental and applied research interest over the last two decades. When ILs are employed in different applications at charged interfaces (*e.g.* in electrochemistry and lubrication), it is imperative that researchers understand the fundamental structure and behaviour of the ions at the electrode (or other charged surfaces) because ion structure can dramatically affect the application performance. While the properties of bulk ILs often define the physical parameters – such as solubilities, viscosities, water uptake, diffusivity etc. – these properties may be altered at the electrode/IL interface because of denser ion structuring in the electrical double layer (EDL) at charged surfaces.

IL ions interact strongly with solid surfaces and usually have pronounced interfacial structures, which can be divided into three distinct regions: the boundary (surface-adsorbed) layer, the transition zone (near-surface layers), and the bulk phase (**Figure 1a**).[1] The boundary layer consists of ions in direct contact with the solid surface, thus the composition of the boundary layer is predominantly determined by the properties of the solid substrate; adjacent to the boundary layer are several near-surface layers, termed the transition zone. Through this transition zone, which is typically a few nanometres across, the pronounced interfacial layer structure decays into the bulk phase.[2-6]

Experimental techniques, such as atomic force microscopy (AFM),[7-8] vibrational sum-frequency generation (SFG) spectroscopy,[9-10] surface force apparatus (SFA),[11] neutron reflectometry (NR),[12] surface-enhanced Raman spectroscopy (SERS),[13] low-energy electron and photoemission electron microscopy,[14] X-ray scattering,[15] capacitance[16] and impedance[13] measurements, as well as theoretical approaches[3, 17-19] have been used to characterize the layering and interfacial structure of ILs close to a surface. For electrochemical applications, the EDL composition at charged surfaces is of crucial importance because electron transfer and charge storage occur within this region. In aqueous electrolytes, the widely accepted Stern-model predicts the potential decay from the electrode towards the bulk electrolyte (see **Figure 1c**).[20]

However, the absence of solvent molecules in ILs results in an ion concentration that oscillates from the innermost ion layer near the surface extending out to the bulk phase (**Figure 1a** and **1b**).[21] At a moderately charged surface, the IL boundary layer is called the Stern layer. It is enriched with a monolayer of counter-ions that "overscreens" the surface charges and thus induces a few near-surface cation or anion layers (**Figure 1a**). At a highly charged surface, the crowding of counter-ions can extend across two monolayers and dominate overscreening (**Figure 1b**). Furthermore, IL cations and anions are much larger than conventional electrolyte salts (e.g. Na^+, K^+, Cl^-), so their charges are more delocalised. The chemical structures of ILs are also much more diverse because they can contain different functional groups, sometimes with polar and non-polar side chains. Therefore, a robust model for the EDL to describe all ILs is still under intense investigation.

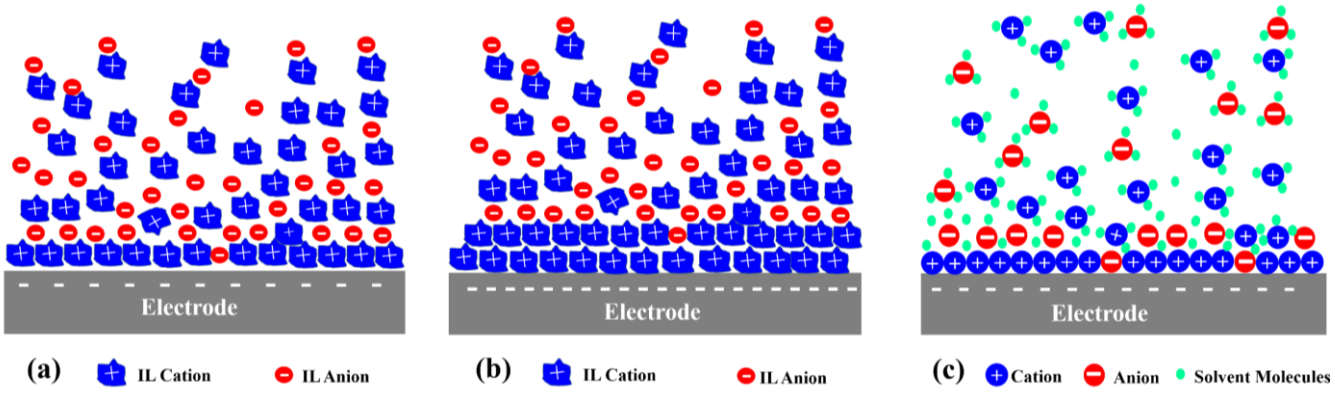

Figure 1. Simplified schematic showing the structure of the double layer for an IL with a short alkyl chain that has homogeneous bulk structure at (a) a low charged surface and (b) a high charged surface *vs* (c) conventional solvents.

The purpose of this Perspective article is to highlight key articles from the last 3 years which probe the relationship between IL interfacial nanostructure for electrochemical and lubrication applications. For more exhaustive descriptions of IL EDLs, the reader is referred to detailed review articles.[2-3] In this Perspective, we will first discuss the important effects of water on the EDL, noting that water can often be present in ILs due to their hygroscopic nature.[22] We will then go on to highlight some of the work done over the last three years where the structure of the IL/electrode interface was deemed to be important, specifically in the different areas of supercapacitors, batteries, sensors and lubrication. It is hoped that this article will provide some background and perspective to the reader on how we believe it is vitally important to consider the

fundamental behaviour of ILs at electrodes and charged surfaces, even in the context of very application-focussed work.

1.1 Effect of Water on the EDL

Water can be a friend or foe in ILs, depending on the application.[23-24] Water absorption in the bulk IL can be deliberately controlled by careful selection of dipole moments of the cation and anion of the IL *i.e.* if a lower content of water in the IL is required, then the cation and anion combinations should be chosen so that they are significantly less polar than water. Water uptake in the bulk IL is believed to be mainly dependent on the anion, because water molecules form more hydrogen bonds with anions rather than with cations.[25-26] Therefore, ILs with more hydrophilic anions, such as $[BF_4]^-$ and $[PF_6]^-$, have higher water solubilities compared with ILs containing more hydrophobic anions, such as $[TFSI]^-$ and $[FAP]^-$.[27]

The electrosorption of incorporated water in the EDL at electrified interfaces is also known to occur in ILs.[28] At gold or carbon electrodes, close to the potential of zero charge, it was reported that water is mainly present in the bulk phase rather than in the interfacial region.[28] As charge is applied to the electrodes, water adsorption increases at both the positively and negatively charged electrodes in hydrophobic ILs such as $[C_4mpyrr][TFSI]$. However, for more hydrophilic ILs such as $[C_4mim][BF_4]$, although water still accumulates at the positively charged electrode, it is more depleted at the negatively charged electrode compared to the neutral electrode.[28] This effect is likely controlled by the nature of anion, where water rather strongly interacts with hydrophilic $[BF_4]^-$ anions, so solvated $[BF_4]^-$ ions are attracted to the positively charged surface (termed 'water following anions'). The same IL/water system was also examined by Harada et al., who showed via frequency-modulation atomic force microscopy (FM-AFM) that even for highly diluted $[C_4mim][BF_4]$ (molar ratio of 0.05 to 0.1 IL in water), accumulation of the IL ions at both the cathode and anode is observed and the coverage is increased by applying a potential.[29]

The operating potential range or "electrochemical windows" of ILs are also very sensitive to changes in humidity levels in the environment above the IL.[30-31] The electrochemical window (EW) of 'dry' ILs is determined by the oxidation and reduction of the anion and cation, respectively; EWs were found to be between *ca.* 4 – 7 V on a Pt surface, depending on the IL structures. However, 'wet' RTILs had very

narrow EWs on Pt between *ca.* 1.5 – 2.5 V,[30] suggesting that the anodic and cathodic limits are determined by the oxidation and reduction of water. Even at very low humidity levels in ILs (as low as 10 % relative humidity), a significant amount of water can be present in the interfacial electrode/RTIL region that reduces the EW.[29-30] Understanding this effect is important because some applications require operation in real environments where moisture will be present at significant levels. In-situ atomic force microscopy (AFM) studies reveal that water electrosorption has a profound impact on the double layer structure near charged and electrified planar surfaces.[32] However, the addition of water largely affects the structure and thickness of the Stern layer (surface adsorbed innermost layer) compared to the layers further away from the electrode. The presence of water in ILs causes reorganization of ions in the Stern layer; the extent of which is mainly dependent on the electrode potential, the electrode material, the chemical structure of the IL and its water content.[22]

To elaborate on the potential dependent molecular rearrangements and phase transitions in the EDL, Sieling *et al.* fabricated a monolayer of amphiphilic imidazolium-based IL on a gold surface and immersed it into an aqueous electrolyte solution.[33] The IL monolayer represents the innermost interfacial layer of the EDL in dilute ILs. Potential driven structure transformations and changes in orientation of the ions were observed using in-situ polarization modulation infrared reflection absorption spectroscopy (PM IRRAS). As the negative charge density increases at the Au electrode, hydrocarbon chains in the IL shift from a bent/tilted orientation to an upward/straightened orientation, allowing more space for ions to reach the electrode surface, while the imidazolium orientation remains unaltered. By using coarse-grained mean-field theory, Chen *et al.* disclosed the phenomenon that when water was present in the ILs, contrasting dielectric properties between species play an important role in water adsorption or depletion near the electrode.[24] Although strong electrostatic correlations between cations and anions can increase double layer capacitance, they do not alter the adsorption phenomenon. Components with higher dielectric constants preferentially adsorb on the electrode; at the same time, charge screening determines if the capacitance is increased or decreased. Hence, both electronic polarizability and electrostatic correlation can modify the

capacitance. This concept can be applied to design electrolytes with preferential adsorption of targeted species onto the electrode.

In-situ sum-frequency generation (SFG) spectroscopy can be used to accurately resolve the interfacial structure and observe potential driven water adsorption at the electrode. SFG investigations of water in [C_2mim][BF_4] at a Pt(111) surface revealed that the electrode potential causes free water molecules from the bulk to form a network of hydrogen-bonded water molecules at the interface (see **Figure 2**).[34] By using water electrosorption as a 'reporter molecule', the authors determined the potential of zero charge (PZC) of Pt in the IL to be +0.1 V *vs* a standard hydrogen electrode (SHE). These diverse studies reveal the complicated behaviour of water at the EDL in ILs, presumably caused by strong bonding interactions with the ions. Therefore, more work is still needed to for a full understanding of the behaviour of water at the electrode-solution interface especially when different IL cations and anions are employed.

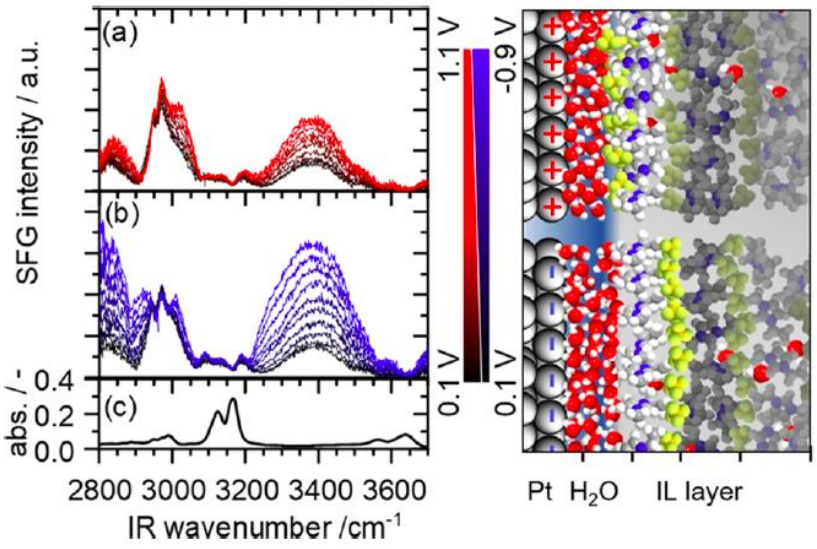

Figure 2. Potentiodynamic in-situ sum-frequency generation (SFG) spectra of the Pt(111)/[C_2mim][BF_4] interface with 0.5 M H_2O. (a) SFG spectra at potentials E > 0.1 V vs SHE and (b) spectra at E < 0.1 V vs SHE. The potential sweep rate was set to 0.9 mV/s. (c) IR absorbance spectra of the bulk [C_2mim][BF_4] electrolyte with 0.5 M H_2O. The right column schematically shows the proposed structures of water and IL ions at the Pt(111) interface. Reprinted with permission from reference [34]. Copyright 2020 American Chemical Society.

The next sections will describe some of the recent developments over the last three years in the areas of supercapacitors, batteries, sensors and lubrication systems where the structure of the EDL is an integral part of the application response. We highlight the importance of considering the EDL structure and

its behaviour as a function of applied potential when ILs are employed for applications in these important areas.

2. Effect of the EDL on Electrochemical Applications of ILs

2.1 Supercapacitors

Supercapacitors store and release charge rapidly during charging and discharging processes. The energy density of supercapacitors is determined by the capacitance of the system and the potential window of the solvent. The energy density of supercapacitors can be enhanced by using electrodes with high surface area and by widening the electrochemical window. Although organic electrolytes offer wide potential windows, at the same time they suffer from inflammability and toxicity. ILs are a safe, high-voltage alternative to traditional electrolytes for use in supercapacitors.

The nature of the electrode, along with its surface chemistry, can affect the EDL structure, which in turn affects the differential capacitance of supercapacitors. Porous electrodes are often used for capacitor and battery applications rather than planar electrodes because they can improve ion and electron storage capacity, and their high surface area can enhance reaction rates and improve mass and charge transfer processes. Porous electrodes have varying morphologies and pore-size distributions, resulting in complex EDL charging by imposing a confined environment and modifying the layered structure compared to planar electrodes.[32, 35] Both classical molecular dynamics (MD) and density functional theory (DFT) simulations reveal that the electrode pore-size distribution should be narrow and that the solvent selection should be made based upon the size of the IL ions (relative to the pore size), and the operating voltage to attain the maximum theoretical capacitance.[36-38]

Role of the IL cation

The chemical structure of the IL affects the ion distribution near a charged electrode and within micropores. MD simulations revealed that changing the cation can significantly alter structure and dynamics of the EDL at various potentials, although the capacitance remains almost unaltered.[39] According to conventional EDL theories, the EDL capacitance for imidazolium ILs is inversely proportional to the

length of the neutral segment (alkyl chain) of the imidazolium cation.[35, 40] An increase in the side-chain length reduces the packing density of counterions at a charged surface, thus affecting the cathode more than the anode. For porous electrodes, capacitance increases with an increase in the alkyl chain length of the imidazolium cation,[35, 41] pointing towards a different EDL due to confinement effects. Capacitance improvements are restricted to small micropores at moderate surface potentials. For sufficiently long alkyl chains, the cations form a bilayer structure due to strong aggregation of the nonpolar chains.[42]

In addition to the length of the alkyl chain, orientational preference and the density of ions in the first layer are important parameters for the potential dependency of differential capacitance (C_d) of ILs.[43] Simulations of quaternary ammonium cation-based ILs with four alkyl groups can help to explain this effect. With up to three butyl chains in an ammonium cation ($[N_{4,4,4,1}]^+$), the orientation of the butyl chains shifts from a parallel to perpendicular direction from the electrode as the potential becomes more negative while C_d decreases (see **Figure 3**, a,b,c). However, when four butyl chains are present (**Figure 3**, d), C_d is still smaller despite there being no change in orientation due to geometric restrictions, pointing towards the densification of quaternary ammonium ions in the first layer.[44]

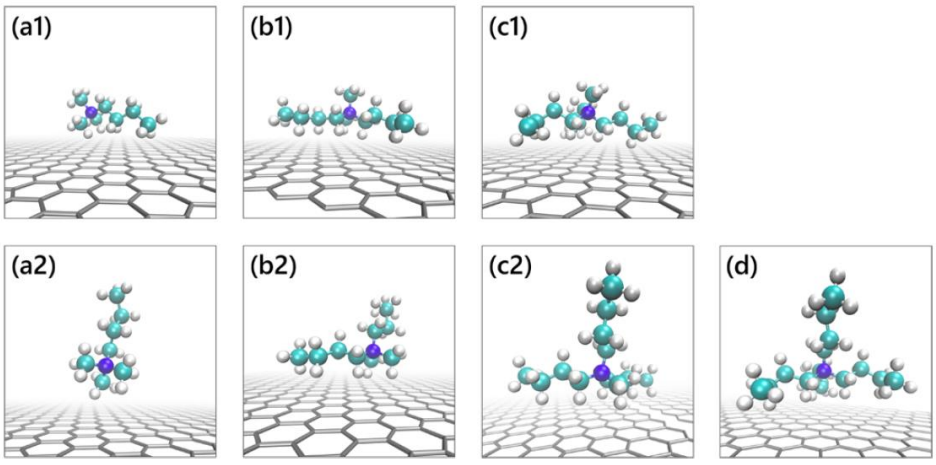

Figure 3. Snapshots of (a) $[N_{4,1,1,1}]^+$, (b) $[N_{4,4,1,1}]^+$, (c) $[N_{4,4,4,1}]^+$, and (d) $[N_{4,4,4,4}]^+$ in the first ionic layer of a negatively charged graphene electrode, viewed from the lateral direction. (1) Lying orientation in which all the butyl chains are parallel to the electrode. (2) Standing orientation in which one or more butyl chains are pointing to the IL bulk. $[N_{4,4,4,4}]^+$ shows the standing orientation only. Reprinted with permission from reference [44]. Copyright 2020 American Chemical Society.

When the alkyl chain length increases to C_8 or more in ammonium based ILs (*e.g.* $[N_{8,8,8,1}]$[TFSI]), steric repulsion dominates ion-ion interactions, which leads to an increase in anion density.[13] At positive

potentials, easy penetration of the large alkyl chain into the anion structure reduces the repulsion between 'like' charges, leading to enhanced capacitance.[13] In the case of a sulphonium based IL, the alkyl chain length affects the dynamic properties but does not affect capacitance at a planar graphene-based supercapacitor device.[45] Comparing the different cations of imidazolium, pyrrolidinium and ammonium, those with more flexible structures show higher capacitance. Ammonium cations show the largest relative increase in capacitance with potential as these ions offer more degrees of rotational freedom and accessibility of larger potentials with a more stable cation.[13]

Role of the RTIL anion

There is no general understanding of whether, or how, the IL anion affects the C_d and the EDL structure in different IL systems, due to the complexity of the electrode-IL interface,[46-47] but Chaban *et al.* reported that ILs with ions of equal sizes showed maximum capacitance.[48] The relationship between anion size and EDL capacitance of the IL was further elaborated by Wang *et al.* who concluded that as anion size increases, ionic mobility is restricted, which in turn increases the EDL thickness, charging time and average differential capacitance at high voltages.[49] In the case of pyrrolidinium ILs with different anions sandwiched between graphene sheets, the range of charge-ordering was found to be highly dependent on the anions. Small sized anions have more electrostatic interactions, enhancing the charge-ordering structures near graphene.[50] However, in imidazolium ILs with cyano-based anions, by varying the number of cyano groups in the anion, the maximum differential capacitance attained at negative potentials remains unaffected. The potential where maximum capacitance occurs shifts to more negative values with an increase in the number of cyano groups on the anion.[51]

Tuneable IL systems

ILs are highly tuneable solvent systems, and many different combinations of ions are possible by changing the chemical structures of the cation and anion and/or adding functional groups. Amino acid ILs (AAILs) are biological ILs that are low-cost, biocompatible and non-toxic. In the case of the AAIL 1-ethyl-3-methyl-imidazolium phenyl alanine ([C_2mim][PHE]), a hydrogen bond exists between the cation and the anion, as

well as between the anions in the bulk state. The number of hydrogen bonds between cations and anions is increased when an AAIL is confined between graphene sheets, while the number of H-bonds between anions remains unaffected.[52] The phenyl ring of the $[PHE]^-$ anion inhibits π-π stacking of the imidazolium cation with graphene, leading to more accumulation of anions in the Stern layer, in contrast to the more commonly used $[C_2mim][PF_6]$ IL, where more cations exist in the first layer. Because the cations and anions in the two ILs have different adsorption and desorption energies from the surface, separation of the anion in the case of an AAIL is easier than the cation, compared to $[C_2mim][PF_6]$. Supercapacitors comprising of AAILs therefore require less energy to show a response to the applied electrical potential.[52] The presence of polar and non-polar groups in the anion of AAILs (and some other conventional ILs) can affect the double layer structure. Polar groups decrease the responding potential even more as they increase the spatial volume of the anion and weaken the anion interaction with graphene. This leads to a more balanced ratio of ions in the first layer.[53] Similar results were reported with an AAIL containing a carboxylic group.[54]

Another more recent class of ILs are surface-active ILs (SAILs), which contain inherent amphiphilic structures that give rise to surfactant-like self-assembly. Mao *et al.* discovered attractions between alkyl chains in the SAIL $[C_4mim][AOT]$, which was found to enhance charge storage at electrified interfaces through the formation of highly ordered nanostructures comprising of distinct polar and non-polar domains that were strongly aligned at the electrode surface (**Figure 4**).[55] However, this was only possible at high temperatures, so the development of SAILs that are more fluid at lower temperatures would be of much benefit for supercapacitor applications.

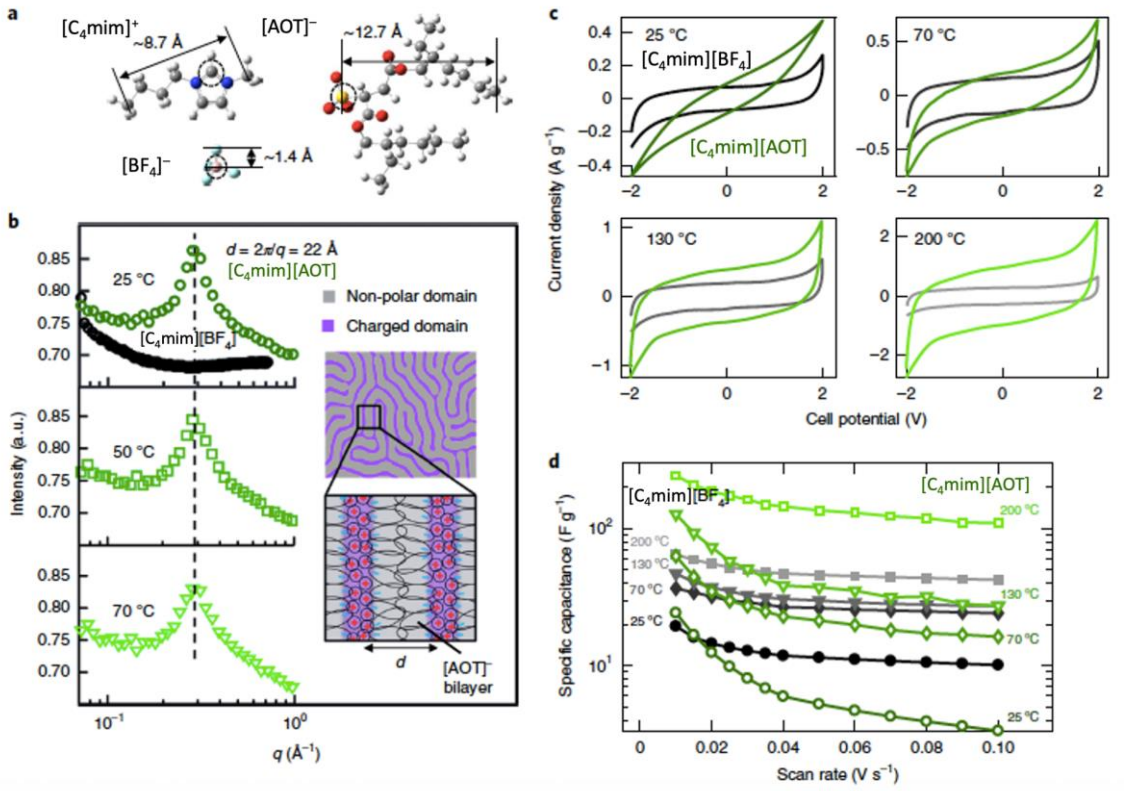

Figure 4. Bulk-phase structural and electrochemical characterization of [C4mim][AOT]. (a) Molecular structures of $[C_4mim]^+$, $[BF_4]^-$ and $[AOT]^-$ (H, white; C, grey; N, blue; S, yellow; O, red; B, pink; F, cyan). Typical distances within the molecular ions are indicated. b, SANS profiles of $[C_4mim][BF_4]$ (25°C) and [C4mim][AOT] (25, 50 and 70°C). Inset: illustration of self-assembly of [C4mim][AOT] leading to a repeating nanostructure comprising $[AOT]^-$ bilayers (red, cation; blue, anion). Simulated SANS profiles are consistent with the experimental data. c, d, Cyclic voltammogram profiles (scan rate = 20 mVs^{-1}) (c) and the specific capacitance versus the scan rate (d) for $[C_4mim][BF_4]$ and [C4mim][AOT] at 25, 70, 130 and 200°C. Reprinted and modified with permission from reference [55]. Copyright 2019 Springer Nature Limited.

IL mixtures

The complex structure of ILs at electrodes can undergo transitions due to composition alteration. Mixing two or more ILs can improve the capacitance as well as the macroscopic properties of the IL as an electrolyte, by modifying ionic electrostatic interactions and ionic steric effects.[56-57] Double salt ILs (containing more than one type of anion or cation) further expands the possibility of different electrolyte compositions as well as ionic interactions, which in turn can tune the EDL properties. In a mixture of two ILs with different sized anions (e.g $[C_2mim][TFSI]/[C_2mim][BF_4]$), the observed enhanced capacitance at the cathode is caused by effective anion exchange, which in turn increases cation adsorption.[37] The extent of this exchange is prominent when smaller sized anions (*e.g.* $[BF_4]^-$) are present at low mole fractions.[37] Wang *et al.* introduced the concept of selective charging by utilizing IL mixtures with different cations on

a porous electrode for high energy and high power density outputs.[58] The difference in ionic interaction leads to selective sieving *i.e.* cations with stronger interactions densely pack into the mesopores, while cations with weak interactions accumulate in the micropores, leading to enhanced capacitance without compromising power density.[58]

Addition of solvents to the IL facilitates ion diffusion and improves the power density of electrical double layer capacitors (EDLCs).[59] An in-depth analysis revealed that solvation dampens charge overscreening, leading to increased capacitance at very low concentrations of solvent.[59] At the same time, solvation decreases the adsorbed ion concentration and this results in a decrease in capacitance in very dilute mixtures. Therefore, careful selection of the solvent and its concentration, together with the electrode surface chemistry, can potentially boost the power density of energy storage devices.[60-61]

2.2 Batteries

Batteries store charge via Faradaic processes. Charging and discharging is accompanied by metal ion intercalation and deintercalation at the cathode and anode, and diffusion of ions in the electrolyte. Because of the diverse and complex irreversible interfacial reactions that include electrolyte decomposition, parasitic reduction of organic cations, solid-electrolyte interphase (SEI) formation and dendritic metal plating, understanding these reactions are crucial to increase the energy density of batteries.[62] IL-based electrolytes are highly desirable for use in high energy density batteries due to their high interfacial stability towards metal anodes and good compatibility with high voltage cathodes. Typically, the IL plays the role of a solvent to dissolve the metal salt. The use of a metal salt with the same anion as the IL, together with the use of an electrode with preferential metal ion intercalation at a relatively lower potential than where organic cation decomposition occurs, can effectively suppress the parasitic reduction of organic cations. Electrolyte decomposition can be avoided by using ILs with large ions and stable functional groups.[63] For example, the low reductive stability of imidazolium (e.g. $[C_2mim]^+$ or $[C_4mim]^+$) can be overcome by replacing the acidic proton with an alkyl group at the C_2-position. Aliphatic quaternary ammonium, phosphonium, or longer chained pyrrolidinium ions (e.g. *N*-alkyl-*N*-methylpyrrolidinium ($[C_nmpyrr]^+$) with $n \geq 4$) can be used instead because they are more electrochemically stable.[64] Furthermore, IL mixtures can increase the

electrochemical stability window by decreasing the potential of zero charge. DFT studies of $[C_2mim][TFSI]/[C_2mim][BF_4]$ mixtures reveal that varying the composition of the mixture results in altered ionic profiles near the electrode surface and hence, a different potential of zero charge.[65] Exploring the optimum composition of IL mixtures and their EDL structures is thus important in this regard.

An insulating solid-electrolyte interphase (SEI) layer formed at the anode and/or cathode because of irreversible electrochemical reactions is highly beneficial to increase the stability of charged electrodes.[63, 66-67] It not only prevents the contact of organic solvent/organic cations with the electrode material, but also allows metal cation intercalation and deintercalation outside the electrochemical stability window of an IL-based electrolyte. Despite its importance, it is the least understood component of Li-ion batteries, and its formation is believed to be related to the initial EDL structure formed at the electrode/solution interface.[68]

The use of a highly concentrated IL electrolyte is beneficial for Li metal batteries.[63, 69] In locally concentrated ILs containing different anions (*e.g.* $[FSI]^-/[TFSI]^-$) with Li salt, the synergy between the anions results in the formation of a highly concentrated SEI, which leads to less dendritic Li plating as well as a higher coulombic efficiency.[63, 66-67] The addition of an electrochemically inert co-solvent such as 1,1,2,2-tetrafluoroethyl 2,2,3,3-tetrafluoropropyl ether (TTE) to the system decreases the viscosity of the electrolyte, while the poor solvating ability of TTE maintains the spatial distribution and solvent structure of the IL ions (see **Figure 5**).[70]

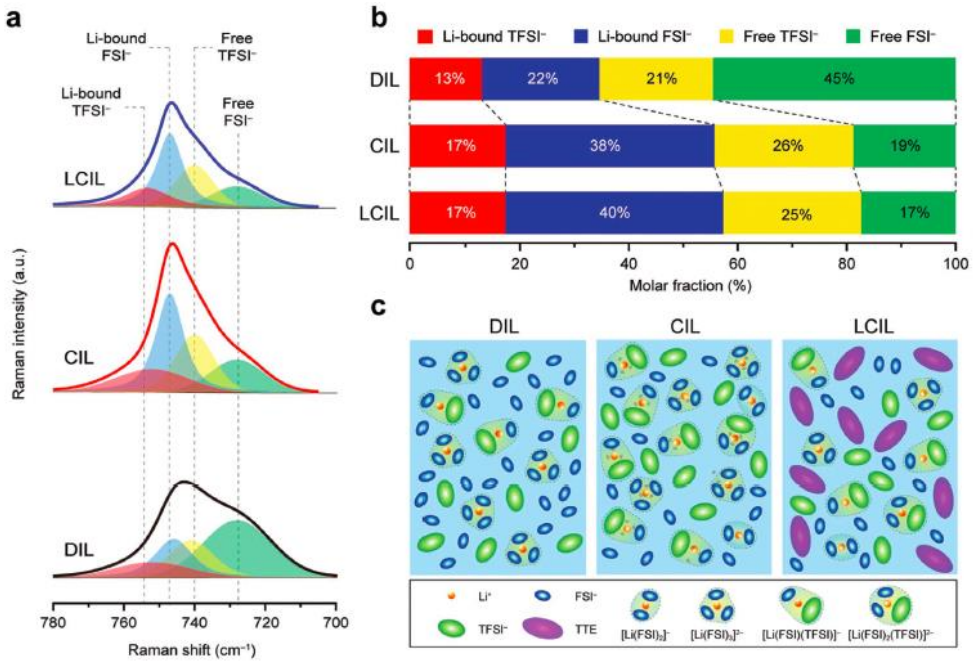

Figure 5. a) Raman spectra and fitting results of dilute IL (DIL), concentrated IL (CIL), and locally concentrated IL (LCIL). b) The mole fractions of the ion species in DIL, CIL, and LCIL determined by Raman measurements. c) Schematic illustration of the solution structures of the IL electrolytes. Reproduced with permission from reference [70]. Copyright 2020 John Wiley and Sons.

For sodium secondary batteries, optimization of sodium salt with the IL gives rise to high performance and good durability at high voltages and over a wide range of temperatures. Hwang *et al.* demonstrated through energy dispersive X-ray (EDX) and X-ray photoelectron spectroscopy (XPS) analysis that decomposition of the IL anion at the cathode leads to the formation of a thin and stable cathode-electrolyte interphase (CEI) which is linked to outstanding performance at high voltage.[71] The choice of the IL anion for Li/Na metal battery applications is crucial in forming the EDL, which determines the stability and passivity of the SEI. ILs containing the dicyanamide ($[DCA]^-$) anion are a cheap alternative to those that contain fluorinated anions ($[PF_6]^-$, $[FSI]^-$, $[TFSI]^-$, $[FTFSI]^-$), but still demonstrate excellent interfacial chemistry for both Li and Na systems. However, the instability of the $[DCA]^-$ anion can lead to passivation of the electrode. Forsyth *et al.* demonstrated that adding Na[DCA], Na[FSI], Na[TFSI], and Na[FTFSI] to a $[C_3mpy]^+$ IL with $[DCA]^-$ can compensate this issue by generating a thicker and stable SEI (see **Figure 6**).[72] An increase in temperature not only decreases the electrochemical stability window, but also affects the thickness of the SEI film.[62, 73] To design a thermally stable SEI, careful choice of the IL, metal salt and electrode is imperative.

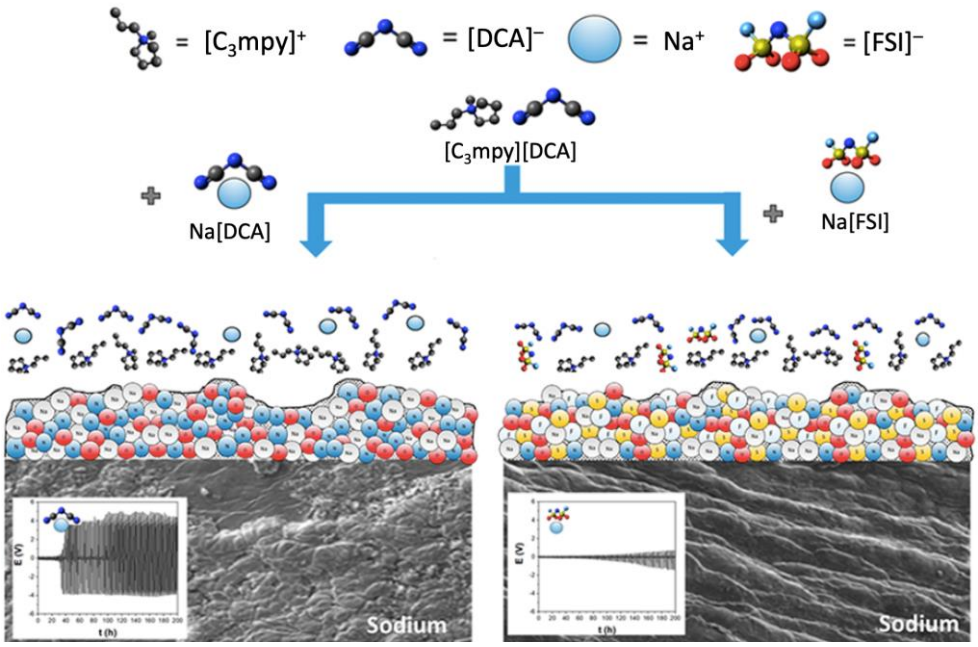

Figure 6. Top: Molecular structures of $[DCA]^-$, $[FSI]^-$, 3-methyl-1-propylpyridinium ($[C_3mpy]^+$) and Na^+ and schematic illustration of SEI formation. Bottom: SEM images of cycled Na surfaces with insets of Na symmetric cells cycled 100 times at 0.1 $mAcm^{-2}$ at 50°C: (left) Na[DCA], (right) Na[FSI]. Modified from the graphical abstract of ref [72] with permission. Copyright 2019 American Chemical Society.

Dendritic growth of metals at the interface is highly undesirable due to the decreased cycle life, and the associated safety risks, including short-circuiting and battery fires. Superconcentrated electrolytes containing an IL and a conventional salt in a 1:1 molar ratio showed markedly different EDLs at electrified electrodes compared to that of the low salt concentration counterpart.[74-75] High salt concentrations lead to more facile reduction of anions and homogeneous metal deposition. Rakov *et al.* demonstrated that preconditioning the electrode with high voltages promotes a larger number of salt aggregates on the cathode and excludes IL cations from realizing a stable SEI formation.[74] Dendrite free Li plating can be achieved through the addition of Na[TFSI] to concentrated Li[FSI] and $[C_2mim][FSI]$ electrolytes. The Na^+ ion stabilizes Li^+ by electrostatically shielding Li^+, which promotes smooth Li deposition by forming passive interphases.[67] Ferdousi *et al*. demonstrated that water (up to 5000 ppm) can be used as an additive for superconcentrated sodium IL electrolytes, which contributes to both stable SEI formation as well as excellent Na cycling stability in these electrolytes.[76] Another strategy is to introduce a heteroatom (*e.g.* Si) substitution in imidazolium based ILs. Si substitution not only decreases the viscosity of the IL, but also imparts a wider electrochemical stability window. When Li^+ salt is added, the presence of Si leads to dendrite free Li deposition at the anode.[77]

In the case of an IL with an aqueous solution containing a salt, different EDLs affect metal cation transfer to the cathode, as well as the morphology of the deposited metal. For example, Begic *et al.*, through molecular dynamics simulation, explained the role of water as an electrochemical catalyst by transferring Zn^{2+} ions through the IL interfacial layers at the cathode.[78] Only 3 wt.% water in 1-ethyl-3-methylimidazolium dicyanamide ([C_2mim][DCA]) containing Zn salt was sufficient to temporarily bind with Zn^{2+} cations and move ions across IL layers to the electrode surface by the constant circular flux of water between the electrode and the bulk IL.[78] Overall, it is clear that the EDL structure of ILs and its effects on battery applications is quite complicated, which can even be true for the simpler conventional systems using electrolyte with organic solvents, where a general consensus is not reached.

2.3 Sensors

For electrochemical (voltammetric/amperometric) sensors, the electron transfer process occurs at the working electrode/electrolyte interface. Therefore, the EDL structure can directly affect the sensitivity and selectivity of chemical sensors[79], and also influence any follow-up reactions after the electrochemical step. The solubility of an "analyte" (the species to be detected), its rate of diffusion towards the electrode, as well as any adsorption processes at the electrode are all determined by the properties of the IL layer close to the electrode. The focus of this discussion will be on the detection of gases, which are the easiest analytes to detect in ILs, because their concentrations can be easily changed by adjusting the concentration of gas in the gas phase above the IL.

Lin *et al.* characterized the IL/electrode interfacial relaxation processes in the context of amperometric gas sensors for oxygen detection.[80] Due to the potential dependency of the interfacial EDL structure, variations in interfacial capacitance were found to occur, and these resulted in difficulties for analyte adsorption at the electrode. Different concentrations of the analyte in the EDL give a change in the response signal. The authors suggested establishing a conditioning potential of 0 V before each measurement for oxygen detection to ensure a consistent and stable IL/electrode interface.[80] Zhan *et al.* showed that the more densely packed EDL of [C_2mim][TFSI] in an electric field shows higher capacitance compared to the less densely packed EDL of [C_4mpyrr][TFSI].[81] They showed that changes in temperature

can alter the behaviour of the EDL in the presence of an analyte, such as carbon dioxide (CO_2). For the electrochemical reduction of CO_2 in [C_2mim][TFSI], five different reaction pathways are possible.[81] Variations in temperature can therefore be used to tune the reaction pathway because of the alteration of the EDL at the IL/electrode interface.

For a sensor to be viable in real environments, it needs to operate over a wide range of temperatures and in different humidity environments. The presence of water/humidity can have a significant influence on the electrochemical mechanism for some gases, such as oxygen. For the oxygen reduction reaction (ORR), the reaction changes from a one-electron mechanism in a 'dry' IL to a two- or four-electron mechanism in a 'wet' IL because of follow-up chemical reactions of the electrogenerated superoxide with water.[82] The change in mechanism results in much larger currents recorded in wet conditions compared to dry conditions. The ORR was studied in a wide range of ILs with different anions and cations, and the IL structure was found to have a very large influence on the ORR currents in humidified conditions.[83] At high humidities, currents increased in ILs according to the tends associated with the bulk solubility of water (up to 6 times current increase for an imidazolium IL with the hydrophilic $[BF_4]^-$ anion). However, at more moderate humidity levels below 40% relative humidity, the cation was found to have the most influence. By keeping the IL anion constant ($[TFSI]^-$) and changing the cation, it was shown that more hydrophilic cations (*e.g.* in $[C_2mim]^+$ or $[C_4mpyrr]^+$) in the EDL can be easily penetrated by water, which can then react with the electrogenerated superoxide radical. However, for much more hydrophobic cations (*e.g.* $[P_{6,6,6,14}]^+$), the dense hydrophobic layer formed at the electrode (due to the presence of long alkyl chains) effectively prevents water molecules from reacting with the electrogenerated superoxide radical in the interfacial region (see **Figure 7a**).[83] This was confirmed by AFM studies that showed that the $[C_2mim]^+$ interfacial structure was obvious in dry conditions (see **Figure 7b**) but collapsed at 40% relative humidity.[83] This shows that for oxygen sensing in moderately humid environments, ILs with very hydrophobic cations are much more favourable than hydrophilic ones, because they can reduce the interactions of superoxide with water. In very wet, water saturated environments (e.g. >60% relative humidity), careful choice of the anion is even more important, with $[FAP]^-$ proving to be the best anion for repelling water near the EDL.[83]

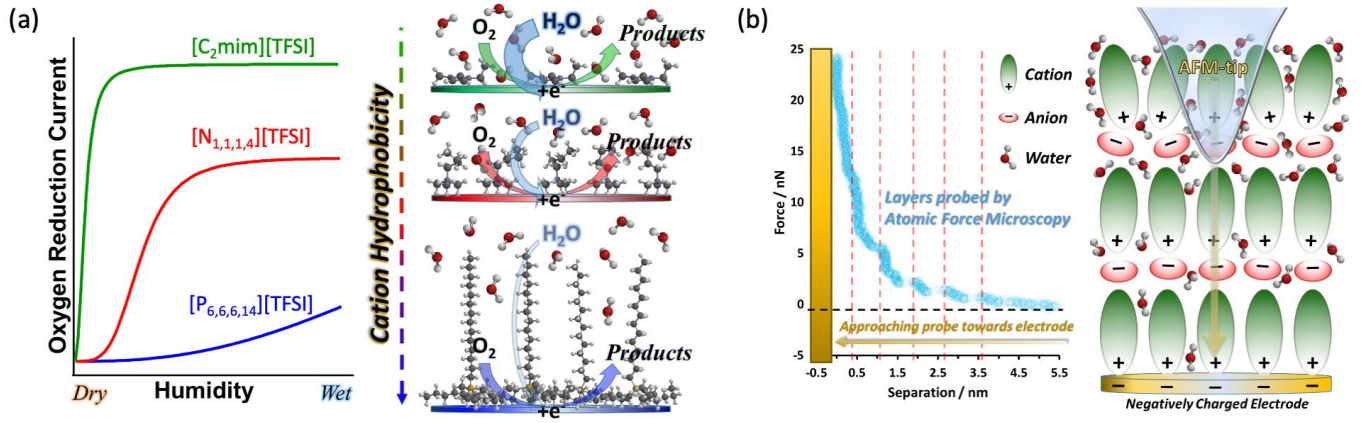

Figure 7. (a) Plot of current vs humidity showing how the normalized ORR current changes with increasing humidity levels in ILs with three different cations. Schematic to the right shows the expected double layer structure, where the small imidazolium and ammonium cations are unable to block water (H_2O) from reaching the electrogenerated superoxide at the electrode. Modified from the graphical abstract of reference [83] with permission. Copyright 2019 American Chemical Society. (b) Force curve generated as an AFM tip approaches a negatively biased electrode, showing distinct jumps that correspond to cation and anion layers normal to the electrode. The right hand side shows a cartoon representation of an AFM tip penetrating through the layers of at the surface. The well-defined layered structure was collapsed in the presence of moisture (40% relative humidity) for the more hydrophilic [C_2mim][TFSI] and [$N_{4,1,1,1}$][TFSI] ILs.

In contrast, the accessibility of water can be also beneficial for sensing. For example, Chi *et al.*[84] showed that trace water in [C_4mpyrr][TFSI] can provide a proton source that facilitates the electrooxidation of acetaldehyde. Tang *et al.*[85] also showed that trace water in ILs is beneficial for the oxidation of carbon monoxide (CO) on a platinum electrode. The IL-platinum interfacial structure of two different RTILs was studied, and changes in the interfacial structure caused a subtle change in the CO oxidation response. However, very high water concentrations hinder CO oxidation, so controlling the water content is very important when detecting this gas.[85]

2.4 Lubrication

Lubricants are applied between sliding surfaces to reduce friction, wear and adhesion.[86] When the normal load is low, the solid surfaces are generally well separated by the bulk lubricant via fluid dynamic forces, friction and wear is relatively low. At high loads, the bulk of the lubricant is squeezed out from the space between the sliding surfaces separated by a single boundary layer of lubricant molecules or ions, which is the EDL Stern layer for a charged surface.[87]

The physical properties of ILs are attractive for the lubrication of a variety of surfaces including – but not limited to – steel, aluminium, titanium and ceramics.[46, 87-89] Similar to conventional high-end lubricants such as perfluoropolyethers, ILs have high mechanical and thermal stability, as well as excellent thermal conductivity, meaning they can transfer heat away from sliding surfaces. In addition, the distinct interfacial nanostructures of ILs make them superior lubricant candidates, especially in the boundary lubrication regime.[90] ILs interact strongly with solid surfaces via electrostatic interactions (if the surface is charged) and van der Waals forces, and laterally with other ions adsorbed to the surface, leading to a well formed, robust boundary (mono)layer.[91] If one of the sliding surfaces is an electrode, the ion composition of the boundary layer can be controlled by applying a potential, and through this the lubricity. This makes trobotronics (the active external control of friction) achievable with ILs. [92-93] As shown in **Figure 8**, the lateral force (friction) change as the compositions of the Stern layers switch from cation-enriched to anion-enriched when the potential changes from negative to positive. Superlubricity, which refers to near zero increase in friction with load, is achieved for (i) $[P_{6,6,6,14}]^+$ enriched Stern layer at -1.0 V, where long alkyl chains associated with $[P_{6,6,6,14}]^+$ cations assist the formation of robust boundary layers via enhancing lateral cohesive forces, and (ii) $[TFSI]^-$ enriched Stern layer at +1.0 V, where the bulky fluorine atoms reduce geometric contact corrugations and form a smooth and flat boundary layer.[93]

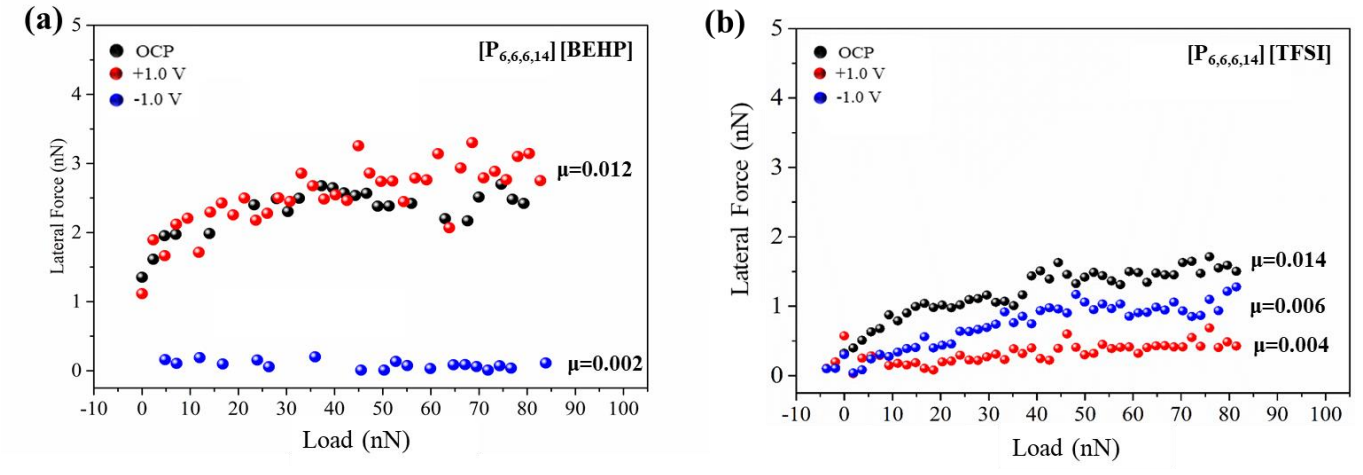

Figure 8. Lateral force vs. normal load of four ILs at the OCP, -1.0 V and +1.0 V on highly oriented pyrolytic graphite: (a) trihexyltetradecylphosphonium bis(2-ethylhexyl)phosphate ($[P_{6,6,6,14}][BEHP]$), (b) trihexyltetradecylphosphonium bis(trifluoromethylsulfonyl)imide ($[P_{6,6,6,14}][TFSI]$). Adapted from reference [93] with permission. Copyright 2021 American Chemical Society.

One key barrier to commercialization of pure ILs as lubricants on a large scale is high cost. However, their tuneable nature means that ILs can be customized to be oil miscible by introducing long alkyl chains to both cations and anions. The development of oil-miscible ILs provides the opportunity to use ILs as lubricant additives, which mitigates the high cost of pure ILs.[86] Compared to commercially available additives such as zinc dialkyldithiophosphates (ZDDPs), ILs generate no ash upon decomposition, they are stable at high temperatures, and have better compatibility with a wider range of surfaces. Previous studies have shown that base oils with low concentrations of IL additives can lubricate a variety of solid surfaces, due to the formation of a robust EDL structure similar with pure ILs.[46] However, the ordering of the ILs in the EDL is weakened to a certain extent due to the existence of oil molecules, which leads to the push-through of the boundary layer and increased friction at high normal load.[94]

Cost-effective tribotronic control of friction is also achievable for IL-oil mixtures. Recent studies show that an ion concentration threshold needs to be reached for IL-oil mixtures to achieve potential-responsive friction, owing to insulation by hydrocarbon base oils.[95] In **Figure 9**, when the IL concentration is 20 wt.%, lower friction at negative potentials occurs due to a densely packed, cation rich Stern layer, whilst higher friction towards positive potentials is found to correlate with a more diffuse, extended anion-rich Stern layer.[95] However, currently the friction-reduction mechanisms for IL-oil tribotronics are still unclear due to the limited research in this area; the compatibility and interaction of ILs with other lubricant additives at applied potentials needs further investigation to develop more high-performing and cost-effective lubrication systems.

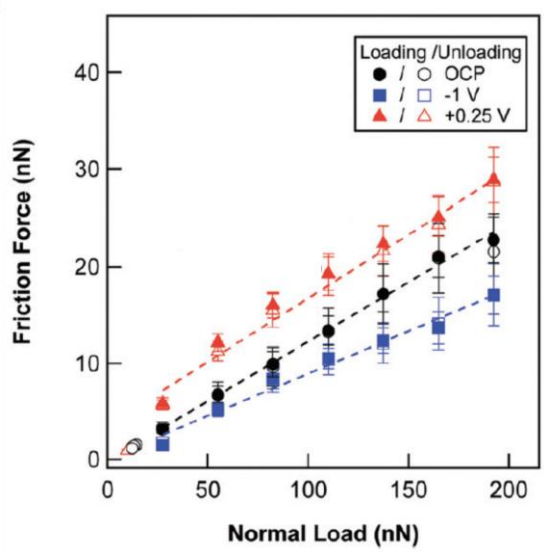

Figure 9. Friction force as a function of normal load in a solution of 20 wt.% IL ([$P_{6,6,6,14}$][BMB]) in propylene carbonate (PC) on a gold electrode surface at three applied potentials (open circuit potential (OCP), -1 V and +0.25 V) during loading (closed symbols) and unloading (open symbols). Adapted from reference [95] with permission from the PCCP Owner Societies.

Summary and Future Outlook

In this Perspective article, we highlighted some key recent reports where the EDL structure of ILs is critical. One beauty of ILs is that the cation and anion structures can be tuned by incorporating different chain lengths and functionalities to give the most favourable properties depending on the application requirements. However, this also presents a challenge to researchers because there are an almost infinite number of combinations of IL cations and anions available, and a lot of research time is therefore required to determine the most optimum IL for the task.

Employing ILs as electrolytes in electrochemical energy storage devices has resulted in considerable improvements in their performance and safety, however, more work is needed before their commercialisation into everyday devices. To increase the energy and power density of IL-based electrochemical energy storage devices, understanding the chemical and interfacial reactions appears to be the key to future success. The selection and manipulation of IL ions, and studying ion-electrode and ion-ion interactions, is a promising way to improve the charge storage capability of supercapacitor and battery devices. For batteries, mitigation of interfacial reactions and the formation of a stable SEI is an efficient approach to widen the electrochemical stability window. Hence, new electrode and IL compositions call for the development of advanced computational simulations and in-situ experimental tools to observe electron-transfer and charge-transfer processes that give real-time data and information.

For applications in gas sensing, a few recent examples have been discussed but further investigations are required. The structure of ILs at electrodes needs to be studied in more detail to explore the benefits, and understand the limitations, for sensing applications. We envision that the tunability of the IL structures will be exploited in future gas sensing applications, where certain chemical moieties can be attached to the cation of anion structure to increase the solubility of gases in the EDL compared to the bulk phase, thus resulting in lower limits of detection and higher sensitivities.

Pure ILs are excellent lubricants for a variety of solid surfaces as they can adsorb strongly to the surface and form robust EDLs. Applying a potential at an electrode surface can tune ion composition and orientation in the EDL, and thus alter the lubricity in the boundary regime. Active control of lubricity via

potential may also be achieved using IL-oil mixtures once a sufficient IL concentration threshold is reached to impart conductivity. The lubricity of such systems strongly depends on the composition and morphology of the boundary (Stern) layers adsorbed on the electrode surfaces, especially at the nanoscale, which have rarely been measured directly *in situ*. Study of ion adsorption kinetics in the EDL will better elucidate the boundary lubrication mechanism. The research outcomes in this area underpin the development of new and cost-effective conductive lubricant systems for advanced applications including smart devices and electric vehicles.

Overall, it is clear that the structure of ions at the electrode is the key to designing favourable electrolytes with the required physical properties for high performing devices incorporating supercapacitors, batteries, sensors, and also for lubrication applications. The authors encourage researchers to further probe into the fundamental properties of the EDL in ILs so that applications with these exciting materials can be widely realised, and we look forward to reading the upcoming experimental and theoretical work in this area.

Notes

The authors declare no competing financial interest.

Acknowledgements

DSS thanks the Australian Research Council (ARC) for funding (Future Fellowship grant number: FT170100315). SD thanks Curtin University for a PhD scholarship. YZ thanks the China Scholarship Council and the Australian Institute of Nuclear Science and Engineering (AINSE) for a PhD scholarship. The authors acknowledge the ARC for funding through a Discovery Project (DP210102119).

Abbreviations

IL	Ionic liquid
RTIL	Room temperature ionic liquid
AFM	Atomic force microscopy
SFG	Vibrational sum-frequency generation spectroscopy
SFA	Surface force apparatus
NR	Neutron reflectrometry
SERS	Surface-enhanced Raman spectroscopy
FM-AFM	Frequency-modulation atomic force microscopy
EDL	Electrical double layer
EDLCs	Electrical double layer capacitors
PM IRRAS	Polarization modulation infrared reflection absorption spectroscopy
PZC	Potential of zero charge
SHE	Standard hydrogen electrode
EW	Electrochemical window
MD	Molecular dynamics simulation
DFT	Density functional theory
C_d	Differential capacitance
AAIL	Amino acid ionic liquid
SAIL	Surface-active ionic liquid
SEI	Solid-electrolyte interphase
EDX	Energy dispersive X-ray
CEI	Cathode-electrolyte interphase
ORR	Oxygen reduction reaction
OCP	Open circuit potential
DIL	Dilute ionic liquid
CIL	Concentrated ionic liquid
LCIL	Locally concentrated ionic liquid
XPS	X-ray photoelectron spectroscopy
SEM	Scanning electron microscopy
$[C_2mim][PF_6]$	1-ethyl-3-methylimidazolium hexafluorophosphate
[C2mim][TFSI]	1-ethyl-3-methylimidazolium bis(trifluoromethylsulfonyl)imide
[C4mpyrr][TFSI]	1-butyl-1-methylpyrrolidinium bis(trifluoromethylsulfonyl)imide
[C4mim][Cl]	1-butyl-3-methylimidazolium chloride
$[C_4mim][BF_4]$	1-butyl-3-methylimidazolium tetrafluoroborate
$[C_4mim][PF_6]$	1-butyl-3-methylimidazolium hexafluorophosphate
[C4mim][TFSI]	1-butyl-3-methylimidazolium bis(trifluoromethylsulfonyl)imide
$[C_5mim][PF_6]$	1-pentyl-3-methylimidazolium hexafluorophosphate
$[MOMIM][PF_6]$	1-[8-mercaptooctyl]-3-methylimidazolium hexafluorophosphate
[C2mim][PHE]	1-ethyl-3-methylimidazolium phenyl alanine
[C2mim][FSI]	1-ethyl-3-methylimidazolium bis(fluorosulfonyl)imide
$[C_2mim][BF_4]$	1-ethyl-3-methylimidazolium tetrafluoroborate
[C2mim][DCA]	1-ethyl-3-methylmidazolium dicyanamide
[C4mim][AOT]	1-butyl-3-methylimidazolium 1,4-bis(2-ethylhexoxy)-1,4-dioxobutane-2-sulfonate
$[N_{8,8,8,1}][TFSI]$	Trioctylmethylammonium bis(trifluoromethylsulfonyl)imide

$[N_{8,2,2,2}][TFSI]$	triethyloctylammonium bis(trifluoromethylsulfonyl)imide
$[N_{888}H][DEHP]$	trioctylammonium bis(2-ethylhexyl)phosphate
$[P_{6,6,6,14}][BMB]$	trihexyltetradecylphosphonium bis(mandelato)borate
$[P_{6,6,6,14}]^+$	trihexyltetradecylphosphonium ion
$[N_{4,1,1,1}]^+$	butyltrimethylammonium ion
$[N_{4,4,1,1}]^+$	dibutyldimethylammonium ion
$[N_{4,4,4,1}]^+$	tributylmethylammonium ion
$[N_{4,4,4,4}]^+$	tetrabutylammonium ion
$[C_3mpy]^+$	3-methyl-1-propylpyridinium
$[C_nmpyrr]^+$	*N*-alkyl-*N*-methylpyrrolidinium ion
$[PF_6]^-$	hexafluorophosphate ion
$[FSI]^-$	bis(fluorosulfonyl)imide ion
$[TFSI]^-$	bis(trifluoromethylsulfonyl)imide ion
$[FTFSI]^-$	fluorosulfonyl (trifluoromethanesulfonyl)imide
$[FAP]^-$	xx
DCA	dicyanamide ion
TTE	1,1,2,2-tetrafluoroethyl 2,2,3,3-tetrafluoropropyl ether
ZDDP	zinc dialkyldithiophosphate
MoDTC	molybdenum dithiocarbamate
PIBSI	Polyisobutene succinimide
PAO_4	Poly alpha olefin 4 cSt base oil
PC	Polycarbonate
CO	Carbon monoxide
CO_2	Carbon dioxide
H_2O	Water

References

1. Li, H.; Niemann, T.; Ludwig, R.; Atkin, R., Effect of Hydrogen Bonding between Ions of Like Charge on the Boundary Layer Friction of Hydroxy-Functionalized Ionic Liquids. *J. Phys. Chem. Lett.* **2020**, *11*, 3905-3910.
2. Hayes, R.; Warr, G. G.; Atkin, R., Structure and Nanostructure in Ionic Liquids. *Chem. Rev.* **2015**, *115*, 6357-6426.
3. Fedorov, M. V.; Kornyshev, A. A., Ionic Liquids at Electrified Interfaces. *Chem. Rev.* **2014**, *114*, 2978-3036.
4. Pinilla, C.; Del Pópolo, M. G.; Kohanoff, J.; Lynden-Bell, R. M., Polarization Relaxation in an Ionic Liquid Confined between Electrified Walls. *J. Phys. Chem. B* **2007**, *111*, 4877-4884.
5. Atkin, R.; Warr, G. G., Structure in Confined Room-Temperature Ionic Liquids. *J. Phys. Chem. C* **2007**, *111*, 5162-5168.
6. Canongia Lopes, J. N. A.; Pádua, A. A. H., Nanostructural Organization in Ionic Liquids. *J. Phys. Chem. B* **2006**, *110*, 3330-3335.
7. Zhou, S.; Panse, K. S.; Motevaselian, M. H.; Aluru, N. R.; Zhang, Y., Three-Dimensional Molecular Mapping of Ionic Liquids at Electrified Interfaces. *ACS Nano* **2020**, *14*, 17515−17523.
8. Fukui, K.-i., Development of Local Analysis Technique of Electric Double Layer at Electrode Interfaces and Its Application to Ionic Liquid Interfaces. *Bull. Chem. Soc. Jpn.* **2018**, *91*, 1210–1219.
9. Romero, C.; Baldelli, S., Sum Frequency Generation Study of the Room-Temperature Ionic Liquids/Quartz Interface. *J. Phys. Chem. B* **2006**, *110*, 6213-6223.
10. Romero, C.; Moore, H. J.; Lee, T. R.; Baldelli, S., Orientation of 1-Butyl-3-Methylimidazolium Based Ionic Liquids at a Hydrophobic Quartz Interface Using Sum Frequency Generation Spectroscopy. *J. Phys. Chem. C* **2007**, *111*, 240-247.
11. Perkin, S., Ionic Liquids in Confined Geometries. *Physical Chemistry Chemical Physics* **2012**, *14*, 5052-5062.
12. Nishi, N.; Uchiyashiki, J.; Ikeda, Y.; Katakura, S.; Oda, T.; Hino, M.; Yamada, N. L., Potential-Dependent Structure of the Ionic Layer at the Electrode Interface of an Ionic Liquid Probed Using Neutron Reflectometry. *J. Phys. Chem. C* **2019**, *123*, 9223−9230.
13. Klein, J. M.; Squire, H.; Gurkan, B., Electroanalytical Investigation of the Electrode–Electrolyte Interface of Quaternary Ammonium Ionic Liquids: Impact of Alkyl Chain Length and Ether Functionality. *J. Phys. Chem. C* **2020**, *124*, 5613–5623.
14. Sitaputra, W.; Stacchiola, D.; Wishart, J. F.; Wang, F.; Sadowski, J. T., In Situ Probing of Ion Ordering at an Electrified Ionic Liquid/Au Interface. *Adv. Mater.* **2017**, *29*, 1606357.
15. Han, M.; Kim, H.; Leal, C.; Negrito, M.; Batteas, J. D.; Espinosa-Marzal, R. M., Insight into the Electrical Double Layer of Ionic Liquids Revealed through Its Temporal Evolution. *Adv. Mater. Interfaces* **2020**, *7*, 2001313.
16. Klein, J. M.; Panichi, E.; Gurkan, B., Potential Dependent Capacitance of [Emim][TFSI], [N1114][TFSI] and [Pyr13][TFSI] Ionic Liquids on Glassy Carbon. *Phys. Chem. Chem. Phys.* **2019**, *21*, 3712--3720.
17. Ivanistsev, V.; O'Connor, S.; Fedorov, M. V., Poly(a)Morphic Portrait of the Electrical Double Layer Ionic Liquids. *Electrochem. Commun.* **2014**, *48*, 61-64.
18. Wu, J.; Jiang, T.; Jiang, D.; Jin, Z.; Henderson, D., A Classical Density Functional Theory for Interfacial Layering of Ionic Liquids. *Soft Matter* **2011**, *7*, 11222-11231.
19. Fedorov, M. V.; Georgi, N.; Kornyshev, A. A., Double Layer in Ionic Liquids: The Nature of the Camel Shape of Capacitance. *Electrochem. Commun.* **2010**, *12*, 296-299.
20. Bard, A. J.; Faulkner, L. R., *Electrochemical Methods: Fundamentals and Applications*; Wiley, 2000.
21. Bazant, M. Z.; Storey, B. D.; Kornyshev, A. A., Double Layer in Ionic Liquids: Overscreening Versus Crowding. *Phys. Chem. Lett.* **2001**, *106*, 046102.

22. Qiao, R., Water at Ionic Liquids-Solid Interfaces. *Curr. Opin. Electrochem.* **2019**, *13*, 11-17.
23. Cui, T.; Lahiri, A.; Carstens, T.; Borisenko, N.; Pulletikurthi, G.; Kuhl, C.; Endres, F., Influence of Water on the Electrified Ionic Liquid/Solid Interface: A Direct Observation of the Transition from a Multilayered Structure to a Double-Layer Structure. *J. Phys. Chem. C* **2016**, *120*, 9341-9349.
24. Chen, H.; An, L.; Nakamura, I., Water Dissolution in Ionic Liquids between Charged Surfaces: Effects of Electric Polarization and Electrostatic Correlation. *Mol. Syst. Des. Eng.* **2018**, *3*, 328-341.
25. Cammarata, L.; Kazarian, S. G.; Salter, P. A.; Welton, T., Molecular States of Water in Room Temperature Ionic Liquids. *Phys. Chem. Chem. Phys.* **2001**, *3*, 5192–5200.
26. Anthony, J. L.; Maginn, E. J.; Brennecke, J. F., Solution Thermodynamics of Imidazolium-Based Ionic Liquids and Water. *J. Phys. Chem. B* **2001**, *105*, 10942–10949.
27. Zhou, T.; Chen, L.; Ye, Y.; Chen, L.; Qi, Z.; Freund, H.; Sundmacher, K., An Overview of Mutual Solubility of Ionic Liquids and Water Predicted by COSMO-RS. *Ind. Eng. Chem. Res.* **2012**, *51*, 6256−6264.
28. Bi, S.; Wang, R.; Lio, S.; Yan, J.; Mao, B.; Kornyshev, A. A.; Feng, G., Minimizing the Electrosorption of Water from Humid Ionic Liquids on Electrodes. *Nat. Commun.* **2018**, *9*, 5222.
29. Harada, T.; Yokota, Y.; Imanishi, A.; Fukui, K.-i., Preferential Formation of Layered Structure of Ionic Liquid at Ionic Liquid Aqueous Solution / Graphite Electrode Interfaces Observed by Frequency-Modulation Atomic Force Microscopy. *e-J. Surf. Sci. Nanotech.* **2014**, *12*, 89–96.
30. Doblinger, S.; Donati, T. J.; Silvester, D. S., Effect of Humidity and Impurities on the Electrochemical Window of Ionic Liquids and Its Implications for Electroanalysis. *J. Phys. Chem. C* **2020**, *124*, 20309-20319.
31. O'Mahony, A. M.; Silvester, D. S.; Aldous, L.; Hardacre, C.; Compton, R. G., Effect of Water on the Electrochemical Window and Potential Limits of Room-Temperature Ionic Liquids. *J. Chem. Eng. Data* **2008**, *53*, 2884-2891.
32. Mendez-Morales, T.; Burbano, M.; Haefele, M.; Rotenberg, B.; Salanne, M., Ion-Ion Correlations across and between Electrified Graphene Layers. *J. Chem. Phys.* **2018**, *148*, 193812.
33. Sieling, T.; Brand, I., In Situ Spectroelectrochemical Investigation of Potential-Dependent Changes in an Amphiphilic Imidazolium-Based Ionic Liquid Film on the Au(111) Electrode Surface. *Chem.ElectroChem* **2020**, *7*, 3233-3243.
34. Kemna, A.; Braunschweig, B. r., Potential-Induced Adsorption and Structuring of Water at the Pt(111) Electrode Surface in Contact with an Ionic Liquid. *J. Phys. Chem. Lett.* **2020**, *11*, 7116-7121.
35. Yang, J.; Lian, C.; Liu, H., Chain Length Matters: Structural Transition and Capacitance of Room Temperature Ionic Liquids in Nanoporous Electrodes. *Chem. Eng. Sci.* **2020**, *227*, 115927.
36. Ma, K.; Zhang, C. H.; Woodward, C. E.; Wang, X., Bridging the Gap between Macroscopic Electrochemical Measurements and Microscopic Molecular Dynamic Simulations: Porous Carbon Supercapacitor with Ionic Liquids. *Electrochim. Acta* **2018**, *289*, 29–38.
37. Fang, A.; Smolyanitsky, A., Simulation Study of the Capacitance and Charging Mechanisms of Ionic Liquid Mixtures near Carbon Electrodes. *J. Phys. Chem. C* **2019**, *123*, 1610–1618.
38. Ers, H.; Lembinen, M.; Mišin, M.; Seitsonen, A. P.; Fedorov, M. V.; Ivaništšev, V. B., Graphene–Ionic Liquid Interfacial Potential Drop from Density Functional Theory-Based Molecular Dynamics Simulations. *J. Phys. Chem. C* **2020**, *124*, 19548–19555.
39. Demir, B.; Searles, D. J., Investigation of the Ionic Liquid Graphene Electric Double Layer in Supercapacitors Using Constant Potential Simulations. *Nanomaterials* **2020**, *10*, 2181.
40. Jo, S.; Park, S.-W.; Shim, Y.; Jung, Y., Effects of Alkyl Chain Length on Interfacial Structure and Differential Capacitance in Graphene Supercapacitors: A Molecular Dynamics Simulation Study. *Electrochim. Acta* **2017**, *247*, 634–645.
41. Gallegos, A.; Lian, C.; Dyatkin, B.; Wu, J., Side-Chain Effects on the Capacitive Behaviour of Ionic Liquids in Microporous Electrodes. *Mol. Phys.* **2019**, *117*, 3603–3613.
42. Watanabe, S.; Pilkington, G. A.; Oleshkevych, A.; Pedraz, P.; Radiom, M.; Welbourn, R.; Glavatskih, S.; Rutland, M. W., Interfacial Structuring of Non-Halogenated Imidazolium Ionic Liquids at Charged Surfaces: Effect of Alkyl Chain Length. *Phys. Chem. Chem. Phys.* **2020**, *22*, 8450-8460.

43. Dong, Y., Effect of Alkyl Chain Length on Interfacial Structure of Imidazolium-Based Tetrafluoroborate Ionic Liquids on Au(100) Electrodes. *Mater. Res. Express* **2020**, *7*, 075010.
44. Katakura, S.; Nishi, N.; Kobayashi, K.; Amano, K.; Sakka, T., Effect of Switching the Length of Alkyl Chains on Electric Double Layer Structure and Differential Capacitance at the Electrode Interface of Quaternary Ammonium-Based Ionic Liquids Studied Using Molecular Dynamics Simulation. *J. Phys. Chem. C* **2020**, *124*, 7873-7883.
45. Sampaioa, A. M.; Fileti, E. E.; Siqueira, L. J. A., Atomistic Study of the Physical Properties of Sulfonium-Based Ionic Liquids as Electrolyte for Supercapacitors. *J. Mol. Liq.* **2019**, *296*, 112065.
46. Cooper, P. K.; Staddon, J.; Zhang, S.; Aman, Z. M.; Atkin, R.; Li, H., Nano-and Macroscale Study of the Lubrication of Titania Using Pure and Diluted Ionic Liquids. *Front. Chem.* **2019**, *7*, 287.
47. Liu, X.; Wang, Y.; Li, S.; Yan, T., Effects of Anion on the Electric Double Layer of Imidazolium-Based Ionic Liquids on Graphite Electrode by Molecular Dynamics Simulation. *Electrochim. Acta* **2015**, *184*, 164–170.
48. Chaban, V. V.; Andreeva, N. A.; Fileti, E. E., Graphene/Ionic Liquid Ultracapacitors: Does Ionic Size Correlate with Energy Storage Performance? *New J. Chem.* **2018**, *42*, 18409-18417
49. Wang, Y.; Qian, C.; Qin, J.; He, H., Molecular Mechanism of Anion Size Regulating the Nanostructure and Charging Process at Ionic Liquid–Electrode Interfaces. *J. Mater. Chem. A* **2020**, *8*, 19908–19916
50. Tsuzuki, S.; Nakamura, T.; Morishita, T.; Shinoda, W.; Seki, S.; Umebayashi, Y.; Ueno, K.; Dokko, K.; Watanabe, M., Effects of Anion on Liquid Structures of Ionic Liquids at Graphene Electrode Interface Analyzed by Molecular Dynamics Simulations. *Batteries & Supercaps* **2020**, *6*, 658-667.
51. Jo, S.; Park, S.-W.; Noh, C.; Jung, Y., Computer Simulation Study of Differential Capacitance and Charging Mechanism in Graphene Supercapacitors: Effects of Cyano-Group in Ionic Liquids. *Electrochim. Acta* **2018**, *284*, 577–586.
52. Razmkhah, M.; Mosavian, M. T. H.; Moosavi, F., Structural Analysis of an Amino Acid Ionic Liquid: Bulk and Electrical Double Layer. *J. Mol. Liq.* **2018**, *268*, 506–516.
53. Razmkhah, M.; Mosavian, M. T. H.; Moosavi, F., What Is the Effect of Polar and Nonpolar Side Chain Group on Bulk and Electrical Double Layer Properties of Amino Acid Ionic Liquids? *Electrochim. Acta* **2018**, *285*, 393–404.
54. Razmkhah, M., Effects of Carboxylic Group on Bulk and Electrical Double Layer Properties of Amino Acid Ionic Liquid. *J. Mol. Liq.* **2020**, *299*, 112158.
55. Mao, X.; Zhang, C. H.; Woodward, C. E.; Wang, X., Self-Assembled Nanostructures in Ionic Liquids Facilitate Charge Storage at Electrified Interfaces. *Nature Materials* **2019**, *18*, 1350-1357.
56. Docampo-Álvarez, B.; Gómez-González, V.; Cabeza, O.; Ivaništšev, V. B.; Gallego, L. J.; Varela, L. M., Molecular Dynamics Simulations of Novel Electrolytes Based on Mixtures of Protic and Aprotic Ionic Liquids at the Electrochemical Interface: Structure and Capacitance of the Electric Double Layer. *Electrochim. Acta* **2019**, *305*, 223–231.
57. Yin, L.; Li, S.; Liu, X.; Yan, T., Ionic Liquid Electrolytes in Electric Double Layer Capacitors. *Sci. China Mater.* **2019**, *62*, 1537–1555.
58. Wang, X.; Mehandzhiyski, A. Y.; Arstad, B.; Van Aken, K. L.; Mathis, T. S.; Gallegos, A.; Tian, Z.; Ren, D.; Sheridan, E.; Grimes, B. A., Selective Charging Behavior in an Ionic Mixture Electrolyte-Supercapacitor System for Higher Energy and Power. *J. Am. Chem. Soc.* **2017**, *139*, 18681-18687.
59. Zhang, Y.; Cummings, P. T., Effects of Solvent Concentration on the Performance of Ionic-Liquid/Carbon Supercapacitors. *ACS Appl. Mater. Interfaces* **2019**, *11*, 42680-42689.
60. Cruz, C.; Ciach, A.; Lomba, E.; Kondrat, S., Electrical Double Layers Close to Ionic Liquid–Solvent Demixing. *J. Phys. Chem. C* **2019**, *123*, 1596-1601.
61. Fang, A.; Smolyanitsky, A., Large Variations in the Composition of Ionic Liquid–Solvent Mixtures in Nanoscale Confinement. *ACS Appl. Mater. Interfaces* **2019**, *11*, 27243-27250.

62. Wang, X.; Salari, M.; Jiang, D.; Chapman Varela, J.; Anasori, B.; Wesolowski, D. J.; Dai, S.; Grinstaff, M. W.; Gogotsi, Y., Electrode Material–Ionic Liquid Coupling for Electrochemical Energy Storage. *Nat. Rev. Mater.* **2020**, *5*, 787–808.
63. Zhang, H.; Qu, W.; Chen, N.; Huang, Y.; Li, L.; Wu, F.; Chen, R., Ionic Liquid Electrolyte with Highly Concentrated LiTFSI for Lithium Metal Batteries. *Electrochim. Acta* **2018**, *285*, 78-85.
64. Jónsson, E., Ionic Liquids as Electrolytes for Energy Storage Applications – a Modelling Perspective. *Energy Storage Mater.* **2020**, *25*, 827–835.
65. Lian, C.; Liu, H.; Wu, J., Ionic Liquid Mixture Expands the Potential Window and Capacitance of a Supercapacitor in Tandem. *J. Phys. Chem. C* **2018**, *122*, 18304–18310.
66. Wang, Z., et al., Highly Concentrated Dual-Anion Electrolyte for Non-Flammable High-Voltage Li-Metal Batteries. *Energy Stor. Mater.* **2020**, *30*, 228-237.
67. Sun, H., et al., High-Safety and High-Energy-Density Lithium Metal Batteries in a Novel Ionic-Liquid Electrolyte. *Adv. Mater.* **2020**, *32*, 2001741.
68. Zhou, Y., et al., Real-Time Mass Spectrometric Characterization of the Solid–Electrolyte Interphase of a Lithium-Ion Battery. *Nat. Nanotechnol.* **2020**, *15*, 224-230.
69. Chen, F.; Forsyth, M., Computational Investigation of Mixed Anion Effect on Lithium Coordination and Transport in Salt Concentrated Ionic Liquid Electrolytes. *J. Phys. Chem. Lett.* **2019**, *10*, 7414-7420.
70. Lee, S.; Park, K.; Koo, B.; Park, C.; Jang, M.; Lee, H.; Lee, H., Safe, Stable Cycling of Lithium Metal Batteries with Low-Viscosity, Fire-Retardant Locally Concentrated Ionic Liquid Electrolytes. *Adv. Funct. Mater.* **2020**, *30*, 2003132.
71. Hwang, J.; Matsumoto, K.; Hagiwara, R., Electrolytes toward High-Voltage $Na_3v_2(Po_4)_2f_3$ Positive Electrode Durable against Temperature Variation. *Adv. Energy Mater.* **2020**, *10*, 2001880.
72. Forsyth, M.; Hilder, M.; Zhang, Y.; Chen, F.; Carre, L.; Rakov, D. A.; Armand, M.; MacFarlane, D. R.; Pozo-Gonzalo, C.; Howlett, P. C., Tuning Sodium Interfacial Chemistry with Mixed-Anion Ionic Liquid Electrolytes. *ACS Appl. Mater. Interfaces* **2019**, *11*, 43093–43106.
73. Horstmann, B.; Single, F.; Latz, A., Review on Multi-Scale Models of Solid-Electrolyte Interphase Formation. *Curr. Opin. Electrochem.* **2019**, *13*, 61–69.
74. Rakov, D. A.; Chen, F.; Ferdousi, S. A.; Li, H.; Pathirana, T.; Simonov, A. N.; Howlett, P. C.; Atkin, R.; M., F., Engineering High-Energy-Density Sodium Battery Anodes for Improved Cycling with Superconcentrated Ionic-Liquid Electrolytes. *Nat. Mater.* **2020**, *19*, 1096–1101.
75. Periyapperuma, K.; Pozo-Gonzalo, C.; MacFarlane, D. R.; Forsyth, M.; Howlett, P. C., High Zn Concentration Pyrrolidinium-Dicyanamide-Based Ionic Liquid Electrolytes for Zn^{2+}/Zn^0 Electrochemistry in a Flow Environment. *ACS Appl. Energy Mater.* **2018**, *1*, 4580–4590.
76. Nie, H.; Schauser, N. S.; Dolinski, N. D.; Hu, J.; Hawker, C. J.; Segalman, R. A.; Read de Alaniz, J. J. A. C. I. E., Light-Controllable Ionic Conductivity in a Polymeric Ionic Liquid. *Angew. Chem. Int. Ed.* **2020**, *59*, 5123-5128.
77. Chen, N.; Guan, Y.; Shen, J.; Guo, C.; Qu, W.; Li, Y.; Wu, F.; Chen, R., Heteroatom Si Substituent Imidazolium-Based Ionic Liquid Electrolyte Boosts the Performance of Dendrite-Free Lithium Batteries. *ACS Appl. Mater. Interfaces* **2019**, *11*, 12154–12160.
78. Begić, S.; Chen, F.; Jónsson, E.; Forsyth, M., Water as a Catalyst for Ion Transport across the Electrical Double Layer in Ionic Liquids. *Phys. Rev. Mater.* **2020**, *4*, 045801.
79. Rehman, A.; Zeng, X., Interfacial Composition, Structure, and Properties of Ionic Liquids and Conductive Polymers for the Construction of Chemical Sensors and Biosensors: A Perspective. *Curr. Opin. Electrochem.* **2020**, *23*, 47-56.
80. Lin, L.; Zhao, P.; Mason, A. J.; Zeng, X., Characterization of the Ionic Liquid/Electrode Interfacial Relaxation Processes under Potential Polarization for Ionic Liquid Amperometric Gas Sensor Method Development. *ACS Sens.* **2018**, *3*, 1126-1134.
81. Zhan, T.; Kumar, A.; Sevilla, M.; Sridhar, A.; Zeng, X., Temperature Effects on CO2 Electroreduction Pathways in an Imidazolium-Based Ionic Liquid on Pt Electrode. *J. Phys. Chem. C* **2020**, *124*, 26094-26105.

82. Khan, A.; Gunawan, C. A.; Zhao, C., Oxygen Reduction Reaction in Ionic Liquids: Fundamentals and Applications in Energy and Sensors. *ACS Sustain. Chem. Eng.* **2017**, *5*, 3698-3715.
83. Doblinger, S.; Lee, J.; Silvester, D. S., Effect of Ionic Liquid Structure on the Oxygen Reduction Reaction under Humidified Conditions. *J. Phys. Chem. C* **2019**, *123*, 10727-10737.
84. Chi, X.; Tang, Y.; Zeng, X., Electrode Reactions Coupled with Chemical Reactions of Oxygen, Water and Acetaldehyde in an Ionic Liquid: New Approaches for Sensing Volatile Organic Compounds. *Electrochim. Acta* **2016**, *216*, 171-180.
85. Tang, Y.; Liu, X.; McMahan, J.; Kumar, A.; Khan, A.; Sevilla, M.; Zeng, X., Adsorption and Electrochemistry of Carbon Monoxide at the Ionic Liquid–Pt Interface. *J. Phys. Chem. B* **2019**, *123*, 4726-4734.
86. Li, W.; Kumara, C.; Luo, H.; Meyer, H. M.; He, X.; Ngo, D.; Kim, S. H.; Qu, J., Ultralow Boundary Lubrication Friction by Three-Way Synergistic Interactions among Ionic Liquid, Friction Modifier, and Dispersant. *ACS Applied Materials & Interfaces* **2020**, *12*, 17077-17090.
87. Cai, M.; Yu, Q.; Liu, W.; Zhou, F., Ionic Liquid Lubricants: When Chemistry Meets Tribology. *Chem. Soc. Rev.* **2020**, *49*, 7753-7818.
88. Ge, X. Y.; Li, J. J.; Wang, H. D.; Zhang, C. H.; Liu, Y. H.; Luo, J. B., Macroscale Superlubricity under Extreme Pressure Enabled by the Combination of Graphene-Oxide Nanosheets with Ionic Liquid. *Carbon* **2019**, *151*, 76-83.
89. Kronberger, M.; Ripoll, M. R.; Dörr, N.; Linhardt, P. J. T. I., In-Situ Cyclic Voltammetry of an Ionic Liquid as a Lubricant Additive in a Steel-Ceramic Contact. *Tribol. Int.* **2020**, *152*, 106264.
90. Perez-Martinez, C. S.; Perkin, S., Interfacial Structure and Boundary Lubrication of a Dicationic Ionic Liquid. *Langmuir* **2019**, *35*, 15444-15450.
91. Niemann, T.; Li, H.; Warr, G. G.; Ludwig, R.; Atkin, R., Influence of Hydrogen Bonding between Ions of Like Charge on the Ionic Liquid Interfacial Structure at a Mica Surface. *J. Phys. Chem. Lett.* **2019**, *10*, 7368-7373.
92. Di Lecce, S.; Kornyshev, A. A.; Urbakh, M.; Bresme, F., Lateral Ordering in Nanoscale Ionic Liquid Films between Charged Surfaces Enhances Lubricity. *ACS Nano* **2020**, *14*, 13256-13267.
93. Zhang, Y.; Rutland, M. W.; Luo, J.; Atkin, R.; Li, H., Potential-Dependent Superlubricity of Ionic Liquids on a Graphite Surface. *J. Phys. Chem. C* **2021**, *125*, 3940-3947.
94. Li, H.; Somers, A. E.; Rutland, M. W.; Howlett, P. C.; Atkin, R., Combined Nano- and Macrotribology Studies of Titania Lubrication Using the Oil-Ionic Liquid Mixtures. *ACS Sustain. Chem. Eng.* **2014**, *4*, 5005–5012.
95. Pilkington, G. A.; Oleshkevych, A.; Pedraz, P.; Watanabe, S.; Radiom, M.; Reddy, A. B.; Vorobiev, A.; Glavatskih, S.; Rutland, M. W., Electroresponsive Structuring and Friction of a Non-Halogenated Ionic Liquid in a Polar Solvent: Effect of Concentration. *Physical Chemistry Chemical Physics* **2020**, *22*, 19162-19171.

Biographies

Debbie Silvester is an Associate Professor and Australian Research Council Future Fellow at the School of Molecular and Life Sciences at Curtin University in Perth. Her research interests include electrochemistry in ionic liquids, understanding electrochemical reaction mechanisms, gas sensing, explosives detection, electrodeposition and formation of modified electrodes for sensing applications. She has published more than 80 journal articles, 2 book chapters and 2 patents and leads a team of researchers in the Electrochemistry & Sensors group at Curtin University.

Rabia Jamil completed her M.Sc at Quaid-i-Azam University, Islamabad, Pakistan. Her M.Phil was carried out in the same university under the supervision of Dr. Muhammad Shahid Ansari, focused on the synthesis of nanomaterials with various surface modifications for electrocatalysis and materials chemistry for renewable energy. She will soon begin PhD under the supervision of A/Prof Debbie Silvester (her start has been delayed due to travel restrictions following COVID-19), focussing on the use of ionic liquids and poly(ionic liquids) for gas sensing and electrochemical applications.

Simon Doblinger is a third year PhD student at Curtin University under the supervision of A/Prof Debbie Silvester. He completed his Masters at the University of Regensburg (Germany) under the supervision of Prof. Werner Kunz and Prof. Jean-Marie Aubry (Ecole Nationale Supérieure de Chimie de Lille, France), focused on the physicochemical and interfacial characterization of complex fluids. His PhD research focuses on the electrochemical gas sensors based on room-temperature ionic liquids and poly(ionic liquids).

Yunxiao Zhang is currently a PhD student at the University of Western Australia under the supervision of Prof. Rob Atkin and Dr Hua Li. His research interests focus on investigating nanotribology and interfacial structure of ionic liquids.

Rob Atkin is a Professor of Chemistry at University of Western Australia, where he leads the Ionic Liquids Group. His research interests span fundamental to applied areas including ionic liquids and deep eutectic solvents, surfactant and polymer adsorption, surface coatings, lubricants, electrolytes, production of biofuels from coal and biomass, microencapsulation, preparation of 2D materials, and protein droplet formation in cells. Rob was awarded his PhD in 2003 and has formerly held an Australian Research Council Postdoctoral Fellowship and Australian Research Council Future Fellowship. He has published over 180 peer reviewed journal articles to date.

Hua Li is a research fellow at University of Western Australia. She received her PhD in Applied Science (Minerals and Materials) from Ian Wark Research Institute, University of South Australia. Her research is focused on dynamic interfacial nanostructure and forces at liquid-solid interfaces. She has published over 50 peer reviewed journal articles to date.

TOC Graphic

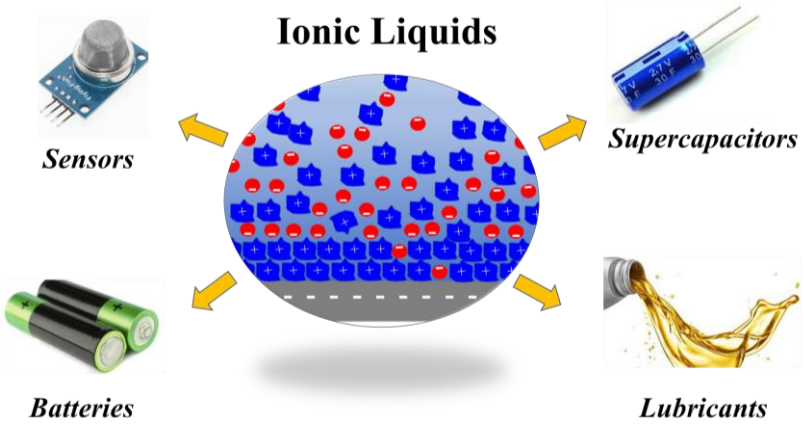
Ionic Liquids
Sensors
Supercapacitors
Batteries
Lubricants